

High-Frequency Ultrasound Characterization Of Pulmonary Arterial Wall Under Normoxic And Hypoxic Conditions*

K. R. Waters

Materials Reliability Division
National Institute of Standards and Technology
Boulder, Colorado, USA
krwaters@boulder.nist.gov

* Official contribution of the National Institute of Standards and Technology; not subject to copyright in the United States.

Abstract—Diagnosis of secondary pediatric pulmonary hypertension is often difficult because no single test permits complete evaluation. Improved understanding of the effects of hypertension on ultrasonic (US) properties of the wall of the pulmonary artery (PA) could lead to earlier detection. High-frequency US *in vitro* measurements were performed on fresh, excised PA walls from normoxic and hypoxic Long-Evans rat models to determine whether US properties differed between groups. Three population groups were studied: six normals, four normal hypoxics, and nine genetically modified (GM) hypoxics. The extrapulmonary artery system (main trunk, left and right branches) was excised following sacrifice and stored on ice in a nutritive solution until measurement. Ultrasonic measurements on the fresh specimens were performed by means of a 50 MHz acoustic microscope in a conventional double-transmission arrangement. The speed of sound (SOS) was determined from differences in times of flight between the reference and tissue measurements. Slope of attenuation was determined from the same signals using a log spectral subtraction technique. An expected increase (up to 10 %) in SOS was observed for the normal hypoxic model compared to the normal model, but an unexpected decrease (by up to 6 %) was observed for the GM hypoxic model. The slope of attenuation in both hypoxic models was greater (by up to 100 %) than that of the normal model.

Keywords—acoustic microscopy; attenuation; hypertension; pulmonary artery; speed of sound; tissue characterization

I. INTRODUCTION

Secondary pulmonary hypertension (PHT) is a potentially fatal complication of congenital heart defects in children, particularly for those who live at high altitude. Discovering the pathophysiology and expression of the disease may lead to improved diagnostics and treatments. We investigate how the ultrasonic properties of the healthy tissues of pulmonary artery and its constituents differ from those of diseased tissue.

The reduced oxygen content in high-altitude environments causes children born with heart defects to have a greater propensity for developing PHT. A long-term goal of the current research is to develop less-invasive diagnostics that might hasten treatment and mitigate permanent damage. At

present, diagnosis is sometimes delayed by two factors: a variety of pathological conditions can display similar clinical expression, and physicians are reluctant to subject a child to catheterization unless it is clearly necessary, because it is an invasive technique [1]. Consequently, a need exists for improved understanding of the ultrasonic properties of the wall of the pulmonary artery (PA).

Quantitative ultrasonic characterization of biological materials involves the application of the measurement techniques of physical acoustics to biological and medical problems. Changes in ultrasonic properties can be correlated with changes in structure and morphology to provide insight into a disease process, for example. A fundamental understanding of the basic acoustic interactions in tissue can enhance the diagnostic utility of ultrasound [2].

The goal is to quantitatively evaluate the ultrasonic properties of normoxic (having normal oxygen content) and hypoxic (having reduced oxygen content) pulmonary arteries and identify structural differences between these populations. We begin with a rat model to determine whether we can detect differences in the ultrasonic properties between conditions. The Long-Evans breed of rats is chosen because it can be genetically modified (GM) so that the endothelin-B receptor is disabled. The endothelin-B receptor is responsible for activating the vasodilators prostacyclin and nitric oxide, which play a role in how an arterial wall responds to changes in the mechanical-stress environment. A low-pressure, reduced-oxygen environment is used to induce PHT.

II. STRUCTURE OF THE PULMONARY ARTERY

The elevated blood pressure in the PA in patients that suffer from secondary PHT leads to remodeling of the PA that causes the heart to work harder, leading to still higher pressures. It is necessary to know both the structure of the PA and how it remodels due to changes in the mechanical-stress environment.

A. Pulmonary Artery

Fig. 1(a) shows a cut-away illustration of an artery. It is the intima, which is in contact with the blood of the lumen, the

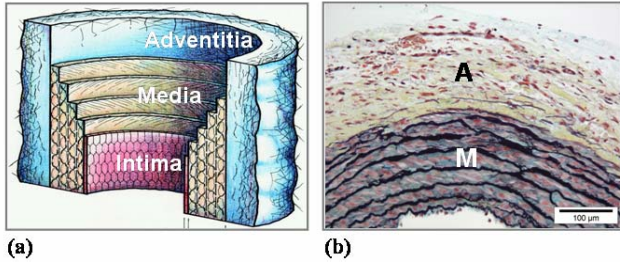


Figure 1. (a) Cut-away illustration of an artery. (b) Optical micrograph of a histologic slice of the pulmonary arterial wall from a hypoxic rat model stained with Pentachrome. A 100 μm scale bar is also included.

media (M) that provides most of the elastic properties of an artery, and the adventitia (A). For purposes of the present study, we are primarily interested in the media. Fig. 1(b) shows an optical micrograph of a histologic slice of the PA wall from a hypoxic rat model. It has been stained with Pentachrome to facilitate identification of certain tissues. The 100 μm scale bar gives a sense of size to these structures. Constituents of normal media include smooth muscle (46 %), collagen (28 %), ground substance (17 %), and elastin (9 %) [3].

B. Remodeling due to Hypertension

The natural development of cells and tissues occurs in a mechanically-stressed environment. Changes in the stress environment can lead to a number of structural and functional changes, including changes in mass and internal structure as well as the building or reabsorption of extracellular structures [4]. This may also modify the ultrasonic properties of the structure. In the case of hypertension, studies have shown that arteries remodel in order to normalize the associated increase in stress. Possible types of remodeling include thickening of media and adventitia and stiffening of the arterial wall. Here, thickening could be due to smooth muscle cell hypertrophy and increased collagen and elastin content.

III. EXPERIMENTAL TECHNIQUE

A. Tissue Specimens and Preparation

Long-Evans rat models are raised at the University of Colorado Health Sciences Center (UCHSC) in Denver. The rat models are sacrificed at 12 – 13 weeks of age, and the extrapulmonary system (main trunk and left and right branches) is excised. The PAs are kept on ice until measurements are performed at the NIST facilities. All measurements are performed within 24 hours of sacrifice.

Three populations of rat models are considered: six normoxic Long-Evans (controls), four hypoxic Long-Evans, and seven genetically-modified (GM) hypoxic Long-Evans. The hypoxic rat models are placed for three weeks in a hypobaric chamber that simulates an altitude of 5200 m. This altitude has roughly half the oxygen content of air at sea level such that the hypoxia presumably induces PHT.

The extrapulmonary system is further prepared prior to ultrasonic measurements. Each arterial section (left branch,

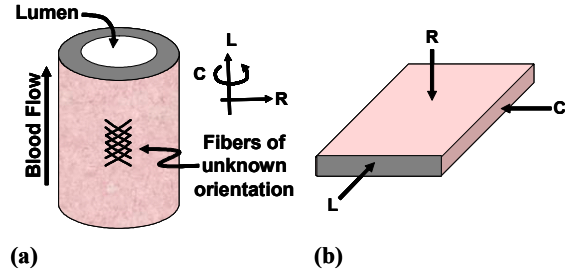


Figure 2. (a) Illustration of the medial layer with fibers of unknown orientation. Here, L is the longitudinal direction, C is the circumferential direction, and R is the radial direction. (b) Illustration of tissue membrane.

right branch, main trunk) is segmented, and the PA wall is cut in the longitudinal direction. The arterial wall is opened as a membrane, and the adventitia is removed under an optical microscope by means of tissue scissors. Measurements on fresh tissue are performed in the radial direction as depicted in Fig. 2(b).

B. Acoustic Microscope

Ultrasonic measurements are performed by means of an acoustic microscope setup with a 50 MHz transducer (6 mm diameter, 13 mm focal length, -6 dB bandwidth of (25 to 65) MHz), as shown in Fig. 3. Tissue specimens are mounted on a stainless steel fixture and immersed in a degassed, nutritive solution heated to 37 $^{\circ}\text{C}$. Motion control and data acquisition are automated.

C. Measurement Protocol

A standard double-transmission technique is employed such that the ultrasound propagates through the tissue from the transducer to the reflector and again from the reflector back to the transducer. The nominal focal plane of the transmitting transducer is at the stainless steel reflector. Reference scans are performed that include only the nutritive solution in the propagation path. The PA tissue is then substituted into the propagation path. Scans in the radial direction of the PA wall are performed over an area of 2 mm \times 3 mm with a step size of 50 μm . Fig. 4 compares a representative optical micrograph and amplitude C-Scan. The ultrasonic radio-frequency (RF) signals are saved to disk at each site for off-line analysis.

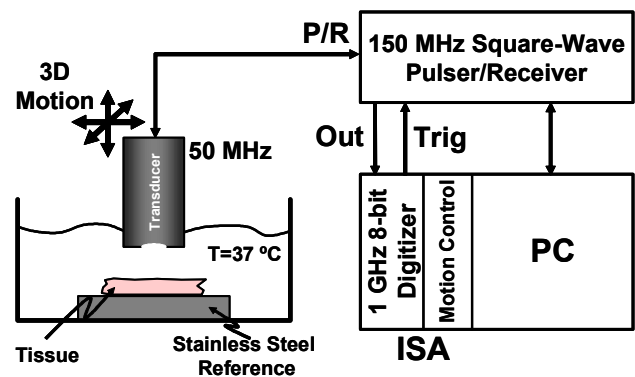


Figure 3. Schematic diagram of acoustic microscope.

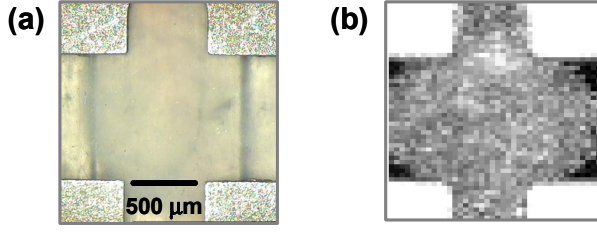


Figure 4. Comparison of (a) an optical micrograph and (b) an acoustic amplitude C-Scan of a pulmonary artery measurement. Tissue clamps shown in the corners of the images keep the tissue in place during measurement. A 500 μm scale bar is shown.

IV. DATA REDUCTION

Analysis is performed at each measurement site within a selected region of interest (ROI) that is generally positioned in the center of a scan region. The ROI is approximately 0.5 mm \times 0.5 mm (10 points \times 10 points).

A. Time-Domain Analysis

Speed of sound (SOS) in the PA tissue is determined from the changes in time of flight of the envelopes of the ultrasonic RF signals for the reference and tissue paths [5]:

$$v_{PA} = v_w \left(1 + \frac{\Delta t_{\text{Shadowing}}}{\Delta t_{PA}} \right), \quad (1)$$

where v_{PA} is the speed of sound in the PA wall, v_w is the temperature-dependent SOS in water [6], $\Delta t_{\text{Shadowing}}$ is the change in time of flight between the shadowed and unshadowed reflector, and Δt_{PA} is the time of flight through the PA tissue.

B. Frequency-Domain Analysis

The attenuation coefficient is determined by spectral analysis of the ultrasonic signals as given by

$$\alpha_{PA}(\omega) = 20 \log_{10} \left(\left| \frac{F_{ref}(\omega)}{F_{PA}(\omega)} \right| \right) / L, \quad (2)$$

where α_{PA} is the attenuation coefficient, F_{ref} is the Fourier transform of the reference path signal, F_{PA} is the Fourier transform of the signal through the PA wall, L is the thickness of the PA wall and was determined from time-domain analysis, and ω is the angular frequency.

V. RESULTS AND DISCUSSION

A. Speed of Sound

The measured SOSs in the radial direction of the left branch, right branch, and main trunk for the normal, normal hypoxic, and GM hypoxic rat models are shown in Fig. 5.

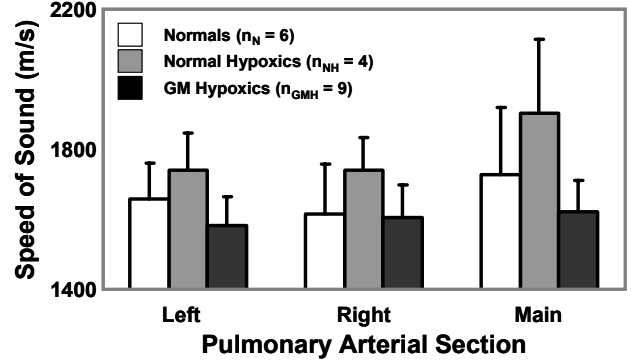


Figure 5. Experimentally measured speed of sound in the radial direction of the pulmonary arterial sections (left branch, right branch, main trunk) for the three rat model populations (normal (N), normal hypoxic (NH), genetically modified hypoxic (GMH)). Standard deviation error bars for each population are included.

Error bars represent the standard deviation between rats for a given population. The radial SOSs in the normal hypoxic models were on average greater than those of the normal models, with the SOS in the main trunk approximately 10% greater. This result is consistent with the hypothesis that hypoxia leads to a stiffening of the artery. However, we observed a decrease in the average SOSs of the GM hypoxic models compared to those of the normal models. This result was unexpected and continues to be a topic of investigation. In addition, we found that SOSs are approximately the same in each PA section of the GM hypoxic model, which differs from the normal and normal hypoxic models.

B. Slope of Attenuation

The measured slopes of attenuation in the radial direction of the left branch, right branch, and main trunk for the normal, normal hypoxic, and GM hypoxic rat models are shown in Fig. 6. Error bars represent the standard deviation between rats for a given population. For all three PA sections, we observed an increased slope of attenuation in the hypoxic models compared to the normoxic model. For the main trunk, the slope of attenuation in the GM hypoxic model was on average approximately 100% greater than that of the normoxic model.

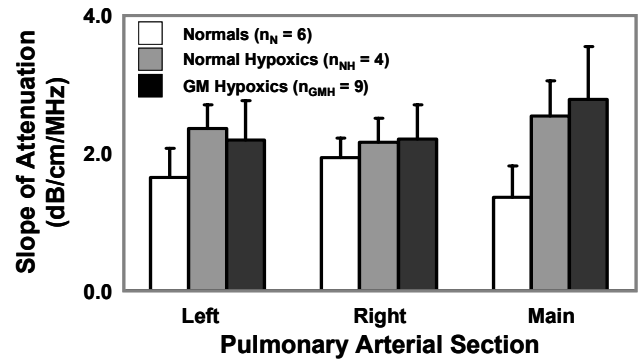


Figure 6. Experimentally measured slope of attenuation in the radial direction of the pulmonary arterial sections (left branch, right branch, main trunk) for the three rat model populations (normal (N), normal hypoxic (NH), genetically modified hypoxic (GMH)). Standard deviation error bars for each population are included.

One could hypothesize that the increase in slope of attenuation is due to collagen deposition [7] during remodeling due to hypoxia, which has been observed in patients with pulmonary hypertension.

C. Comments on Mechanical Testing

This study is part of an investigation to understand both the ultrasonic and mechanical properties of the PA wall under normoxic and hypoxic conditions. Mechanical measurements of the same PA specimens using a bubble-inflation technique [8] were performed in conjunction with the ultrasonic measurements. This technique involves large strain deformation of the PA wall. In developing the ultrasound and mechanical testing protocol, it was necessary to know whether the mechanical testing affected the ultrasonic properties of the PA specimens. Ultrasonic measurements were performed immediately before and immediately after mechanical testing. Preliminary results indicated that mechanical testing affects the SOS only modestly (<5 %), but can cause a decrease in the slope of attenuation of up to 20 %. Consequently, it was determined that all ultrasonic measurements of the specimens would be performed prior to mechanical testing.

VI. CONCLUSIONS

We have performed high-frequency *in vitro* ultrasound measurements on fresh pulmonary arterial walls excised from control and hypoxic rat models. The Long-Evans rat model was chosen for the study of pulmonary hypertension because it can be genetically modified to give the rat a greater propensity for developing hypertension. We observed an expected increase in the radial speed of sound for the normal hypoxic rat models, but an unexpected decrease for the genetically modified rat models when compared to the control rat model. The radial speed of sound of the main trunk of the normal hypoxic model was on average greater by 10 % than that of the control model. We also observed an increase in the slope of attenuation of up to 100 % in the radial direction of the hypoxic rat models compared to the normoxic rat model. Continuing efforts aim to understand the unexpected decrease in radial stiffness of the genetically modified hypoxic rat models, to assess the statistical significance of differences in ultrasonic properties between the rat models, and to correlate changes in the ultrasonic properties with tissue remodeling.

ACKNOWLEDGMENT

The authors thank Elizabeth Drexler (NIST) for discussions on pulmonary hypertension, Chris McCowan (NIST) for tissue preparation, Lonn Rodine (NIST) for design of tissue fixture, Kelley Colvin at the University of Colorado Health Sciences Center (UCHSC) for rat model preparation, and Carlyne Cool (UCHSC) for histologic analysis. This research was performed while the author held a National Research Council Research Associateship Award at the National Institute of Standards and Technology. Animal studies were performed following institutional guidelines and an approved protocol (IACUC 44404001061E).

REFERENCES

- [1] R. Shandas, C. Weinberg, D. D. Ivy, E. Nicol, C. G. DeGroot, et al., "Development of a noninvasive ultrasound color M-mode means of estimating pulmonary vascular resistance in pediatric pulmonary hypertension: mathematical analysis, in vitro validation, and preliminary clinical studies," *Circ.*, vol. 104, pp. 908-913, 2001.
- [2] K. K. Shung, "Introduction," in *Ultrasonic Scattering in Biological Tissues*, K. K. Shung and G. A. Thieme, Eds. Boca Raton, Florida: CRC Press, 1993, pp. 1-18.
- [3] Y. C. Fung, *Biomechanics: Mechanical Properties of Living Tissues*, 2nd ed, New York: Springer-Verlag, 1993, pp. 322-326.
- [4] ---, *Biomechanics: Mechanical Properties of Living Tissues*, 2nd ed, New York: Springer-Verlag, 1993, pp. 369-370.
- [5] B. D. Sollish, "A Device for Measuring Ultrasonic Propagation Velocity in Tissue," in *Ultrasonic Tissue Characterization II*, edited by M. Linzer, U.S. Government Printing Office Spec. Publ. 525, Washington, D.C., 1979, pp. 53-56.
- [6] V. A. Del Grosso and C. W. Mader, "Speed of Sound in Pure Water," *J. Acoust. Soc. Am.*, vol. 52, pp. 1442-1446, 1972.
- [7] C. S. Hall, C. L. Dent, M. J. Scott, and S. A. Wickline, "High-Frequency Ultrasound Detection of the Temporal Evolution of Protein Cross Linking in Myocardial Tissue," *IEEE Trans. Ultrason. Ferroelec. Freq. Contr.*, vol. 47, pp. 1051-1058, 2000.
- [8] E. S. Drexler, A. J. Slifka, J. E. Wright, C. N. McCowan, D. S. Finch, et al., "An Experimental Method for Measuring Mechanical Properties of Rat Pulmonary Arteries Verified With Latex," *J. Res. Natl. Inst. Stand. Technol.*, vol. 108, pp. 183-191, 2003.